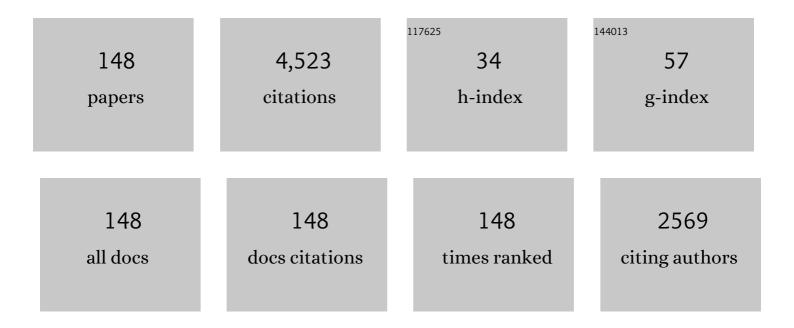
Simone Hochgreb

List of Publications by Year in descending order

Source: https://exaly.com/author-pdf/1049321/publications.pdf Version: 2024-02-01



#	Article	IF	CITATIONS
1	An Overview of Hydrocarbon Emissions Mechanisms in Spark-Ignition Engines. , 0, , .		216
2	Rapid Compression Machines: Heat Transfer and Suppression of Corner Vortex. Combustion and Flame, 1998, 114, 531-545.	5.2	182
3	Advances in rapid compression machine studies of low- and intermediate-temperature autoignition phenomena. Progress in Energy and Combustion Science, 2017, 63, 1-78.	31.2	180
4	The structure of turbulent stratified and premixed methane/air flames II: Swirling flows. Combustion and Flame, 2012, 159, 2912-2929.	5.2	136
5	The structure of turbulent stratified and premixed methane/air flames I: Non-swirling flows. Combustion and Flame, 2012, 159, 2896-2911.	5.2	136
6	Diesel Engine Combustion of Biomass Pyrolysis Oils. Energy & amp; Fuels, 2000, 14, 260-274.	5.1	130
7	Measurements of laminar flame speeds of liquid fuels: Jet-A1, diesel, palm methyl esters and blends using particle imaging velocimetry (PIV). Proceedings of the Combustion Institute, 2011, 33, 979-986.	3.9	129
8	Effects of preferential transport in turbulent bluff-body-stabilized lean premixed CH4/air flames. Combustion and Flame, 2012, 159, 2563-2575.	5.2	129
9	Plasma Reforming of Methane. Energy & Fuels, 1998, 12, 11-18.	5.1	117
10	The nonlinear heat release response of stratified lean-premixed flames to acoustic velocity oscillations. Combustion and Flame, 2011, 158, 2482-2499.	5.2	98
11	Application of Raman/Rayleigh/LIF diagnostics in turbulent stratified flames. Proceedings of the Combustion Institute, 2009, 32, 945-953.	3.9	97
12	Nonlinear dynamics of a self-excited thermoacoustic system subjected to acoustic forcing. Proceedings of the Combustion Institute, 2015, 35, 3229-3236.	3.9	89
13	Mechanisms of Particulate Matter Formation in Spark-Ignition Engines. 1. Effect of Engine Operating Conditions. Environmental Science & Technology, 1999, 33, 3957-3967.	10.0	87
14	Mapping the parameter space for direct-spun carbon nanotube aerogels. Carbon, 2019, 146, 789-812.	10.3	86
15	Large-eddy simulation of pulverized coal jet flame – Effect of oxygen concentration on NO formation. Fuel, 2015, 142, 152-163.	6.4	79
16	Measurements of laminar flame speeds of acetone/methane/air mixtures. Combustion and Flame, 2011, 158, 490-500.	5.2	77
17	Hydrogen autoignition at pressures above the second explosion limit (0.6-4.0 MPa). International Journal of Chemical Kinetics, 1998, 30, 385-406.	1.6	73
18	Time-resolved laser-induced incandescence of soot: the influence of experimental factors and microphysical mechanisms. Applied Optics, 2003, 42, 5577.	2.1	71

#	Article	IF	CITATIONS
19	Experimental measurements of geometric properties of turbulent stratified flames. Proceedings of the Combustion Institute, 2009, 32, 1763-1770.	3.9	69
20	Measurements of triggering and transient growth in a model lean-premixed gas turbine combustor. Combustion and Flame, 2012, 159, 1215-1227.	5.2	67
21	Flow field measurements of a series of turbulent premixed and stratified methane/air flames. Combustion and Flame, 2013, 160, 2017-2028.	5.2	65
22	The structure of premixed and stratified low turbulence flames. Combustion and Flame, 2011, 158, 935-948.	5.2	64
23	Time-resolved laser-induced incandescence and laser elastic-scattering measurements in a propane diffusion flame. Applied Optics, 2001, 40, 2443.	2.1	63
24	Impact of Biomass Pyrolysis Oil Process Conditions on Ignition Delay in Compression Ignition Engines. Energy & Fuels, 2002, 16, 552-561.	5.1	57
25	Spray flame structure of rapeseed biodiesel and Jet-A1 fuel. Fuel, 2014, 115, 551-558.	6.4	55
26	A comprehensive study on CH2O oxidation kinetics. Combustion and Flame, 1992, 91, 257-284.	5.2	50
27	Multiply conditioned analyses of stratification in highly swirling methane/air flames. Combustion and Flame, 2013, 160, 322-334.	5.2	46
28	Spray Combustion Characteristics of Palm Biodiesel. Combustion Science and Technology, 2012, 184, 1093-1107.	2.3	45
29	Laser diagnostics of pulverized coal combustion in O2/N2 and O2/CO2 conditions: velocity and scalar field measurements. Experiments in Fluids, 2015, 56, 1.	2.4	43
30	Flame structure, spectroscopy and emissions quantification of rapeseed biodiesel under model gas turbine conditions. Applied Energy, 2017, 185, 1383-1392.	10.1	43
31	Mechanisms of Particulate Matter Formation in Spark-Ignition Engines. 3. Model of PM Formation. Environmental Science & Technology, 1999, 33, 3978-3992.	10.0	42
32	Mechanisms of Particulate Matter Formation in Spark-Ignition Engines. 2. Effect of Fuel, Oil, and Catalyst Parameters. Environmental Science & Technology, 1999, 33, 3968-3977.	10.0	41
33	Flame Imaging of Gas-Turbine Relight. AIAA Journal, 2010, 48, 1916-1927.	2.6	40
34	The behaviour of laminar stratified methane/air flames in counterflow. Combustion and Flame, 2013, 160, 1070-1082.	5.2	40
35	The effect of fuel volatility on sprays from high-pressure swirl injectors. Proceedings of the Combustion Institute, 1998, 27, 1865-1871.	0.3	36
36	Flow field measurements of pulverized coal combustion using optical diagnostic techniques. Experiments in Fluids, 2013, 54, 1.	2.4	36

#	Article	IF	CITATIONS
37	High spatial resolution laser cavity extinction and laser-induced incandescence in low-soot-producing flames. Applied Physics B: Lasers and Optics, 2015, 120, 469-487.	2.2	36
38	Explosion hazards of aluminum finishing operations. Journal of Loss Prevention in the Process Industries, 2018, 51, 84-93.	3.3	36
39	A comparative analysis of flame surface density metrics inpremixed and stratified flames. Proceedings of the Combustion Institute, 2011, 33, 1419-1427.	3.9	35
40	Decomposition of 1,3,5-trioxane at 700-800 K. The Journal of Physical Chemistry, 1992, 96, 295-297.	2.9	34
41	Conditional analysis of turbulent premixed and stratified flames on local equivalence ratio and progress of reaction. Combustion and Flame, 2015, 162, 3896-3913.	5.2	33
42	Effect of mixture flow stratification on premixed flame structure and emissions under counter-rotating swirl burner configuration. Applied Thermal Engineering, 2016, 105, 905-912.	6.0	33
43	Early Spray Development in Gasoline Direct-Injected Spark Ignition Engines. , 1998, , .		29
44	Detection of direct and indirect noise generated by synthetic hot spots in a duct. Journal of Sound and Vibration, 2017, 394, 220-236.	3.9	29
45	The Effects of Small-Scale Mixing Models on the Prediction of Turbulent Premixed and Stratified Combustion. Combustion Science and Technology, 2010, 182, 1141-1170.	2.3	28
46	The response of stratified swirling flames to acoustic forcing: Experiments and comparison to model. Proceedings of the Combustion Institute, 2015, 35, 3309-3315.	3.9	28
47	Effects of Fuel Volatility and Operating Conditions on Fuel Sprays in DISI Engines: (1) Imaging Investigation. , 0, , .		27
48	Effects of Nonuniform Reactant Stoichiometry on Thermoacoustic Instability in a Lean-Premixed Gas Turbine Combustor. Combustion Science and Technology, 2012, 184, 608-628.	2.3	27
49	Temperature measurements of the bluff body surface of a Swirl Burner using phosphor thermometry. Combustion and Flame, 2014, 161, 2842-2848.	5.2	27
50	Combustion-Related Emissions in SI Engines. , 1998, , 118-170.		26
51	Autonomous extraction of optimal flame fronts in OH planar laser-induced fluorescence images. Applied Optics, 2009, 48, 3866.	2.1	26
52	Extracting flame describing functions in the presence of self-excited thermoacoustic oscillations. Proceedings of the Combustion Institute, 2017, 36, 3851-3861.	3.9	26
53	EFFECT OF ATOMIZING AIR FLOW ON SPRAY ATOMIZATION OF AN INTERNAL-MIX TWIN-FLUID ATOMIZER. Atomization and Sprays, 2015, 25, 657-673.	0.8	26
54	Analysis of the Piston Ring/Liner Oil Film Development During Warm-Up for an SI-Engine. Journal of Engineering for Gas Turbines and Power, 2001, 123, 109-116.	1.1	25

#	Article	IF	CITATIONS
55	A generalised model for acoustic and entropic transfer function of nozzles with losses. Journal of Sound and Vibration, 2019, 440, 212-230.	3.9	23
56	Investigation of the Dilution Process for Measurement of Particulate Matter from Spark-Ignition Engines. , 0, , .		22
57	Quantitative shearography in axisymmetric gas temperature measurements. Optics and Lasers in Engineering, 1999, 31, 21-39.	3.8	22
58	Soot volume fraction measurements over laminar pool flames of biofuels, diesel and blends. Proceedings of the Combustion Institute, 2019, 37, 877-884.	3.9	22
59	Effects of Fuel Volatility and Operating Conditions on Fuel Sprays in DISI Engines: (2) PDPA Investigation. , 2000, , .		21
60	Igniter-induced hybrids in the 20-l sphere. Journal of Loss Prevention in the Process Industries, 2017, 49, 348-356.	3.3	21
61	Direct and Indirect Noise Generated by Entropic and Compositional Inhomogeneities. Journal of Engineering for Gas Turbines and Power, 2018, 140, .	1.1	21
62	Numerical Simulation of Post-Flame Oxidation of Hydrocarbons in Spark Ignition Engines. , 0, , .		20
63	Discrete multicomponent model for biodiesel spray combustion simulation. Fuel, 2014, 126, 44-54.	6.4	20
64	Particulate Matter Emission During Start-up and Transient Operation of a Spark-Ignition Engine (2): Effect of Speed, Load, and Real-World Driving Cycles. , 2000, , .		19
65	Spray and combustion characteristics of biodiesel: Non-reacting and reacting. International Biodeterioration and Biodegradation, 2015, 102, 353-360.	3.9	19
66	Theory and application of reverberated direct and indirect noise. Journal of Fluid Mechanics, 2017, 819, 435-464.	3.4	19
67	Mind the gap: Turbulent combustion model validation and future needs. Proceedings of the Combustion Institute, 2019, 37, 2091-2107.	3.9	19
68	The Roles of Chemistry and Diffusion on Hydrocarbon Post-Flame Oxidation. Combustion Science and Technology, 1997, 130, 365-398.	2.3	18
69	Temperature and water measurements in flames using 1064Ânm Laser-Induced Grating Spectroscopy (LIGS). Combustion and Flame, 2019, 205, 336-344.	5.2	18
70	A Simple Method for Measuring Fine-to-Ultrafine Aerosols Using Bipolar Charge Equilibrium. ACS Sensors, 2020, 5, 447-453.	7.8	17
71	Spray Flame Study Using a Model Gas Turbine Swirl Burner. Applied Mechanics and Materials, 2013, 316-317, 17-22.	0.2	16
72	Planar 2-color time-resolved laser-induced incandescence measurements of soot in a diffusion flame. Aerosol Science and Technology, 2017, 51, 1345-1353.	3.1	16

#	Article	IF	CITATIONS
73	Soot measurement in diluted methane diffusion flames by multi-pass extinction and laser-induced incandescence. Combustion and Flame, 2018, 192, 224-237.	5.2	16
74	Laser-induced incandescence particle image velocimetry (LII-PIV) for two-phase flow velocity measurement. Experiments in Fluids, 2018, 59, 1.	2.4	16
75	Modelling the effect of aerosol polydispersity on unipolar charging and measurement in low-cost sensors. Journal of Aerosol Science, 2019, 130, 10-21.	3.8	16
76	Autoignition of Alcohols and Ethers in a Rapid Compression Machine. , 0, , .		15
77	Extent of Oxidation of Hydrocarbons Desorbing from the Lubricant Oil Layer in Spark-ignition Engines. , 0, , .		15
78	Time, Space, and Species Resolved Measurements of Engine-Out Hydrocarbon Emissions from Spark-Ignited Engines. Combustion Science and Technology, 1997, 127, 333-362.	2.3	15
79	Forced and Self-Excited Instabilities From Lean Premixed, Liquid-Fuelled Aeroengine Injectors at High Pressures and Temperatures. , 2013, , .		15
80	Favre- and Reynolds-averaged velocity measurements: Interpreting PIV and LDA measurements in combustion. Proceedings of the Combustion Institute, 2015, 35, 3803-3811.	3.9	15
81	Reconciling turbulent burning velocity with flame surface area in small-scale turbulence. Journal of Fluid Mechanics, 2019, 858, .	3.4	15
82	Chemical kinetic modeling of exhaust hydrocarbon oxidation. Combustion and Flame, 1995, 100, 193-201.	5.2	14
83	Simultaneous, two-camera, 2D gas-phase temperature and velocity measurements by thermographic particle image velocimetry with ZnO tracers. Experiments in Fluids, 2017, 58, 1.	2.4	14
84	Liquid Fuel Impingement on the Piston Bowl of a Direct-Injection, Spark-Ignited (DISI) Engine under Stratified Operation. , 2001, , .		13
85	Fuel Distribution and Combustion Characteristics in a Direct-Injection, Spark-Ignited (DISI) Engine Under Stratified Operation. , 0, , .		13
86	Relight Imaging at Low Temperature, Low Pressure Conditions. , 2008, , .		13
87	Planar Laser-Induced Fluorescence Fuel Imaging During Gas-Turbine Relight. Journal of Propulsion and Power, 2013, 29, 961-974.	2.2	13
88	The oxidation of CH2O in the intermediate temperature range (943–995 K). Proceedings of the Combustion Institute, 1991, 23, 171-177.	0.3	12
89	Modelling of direct ultraviolet photoionization and charge recombination of aerosol nanoparticles in continuous flow. Journal of Applied Physics, 2017, 121, 023104.	2.5	12
90	Quantification of carbon particulates produced under open liquid pool and prevaporised flame conditions: Waste cooking oil biodiesel and diesel blends. Fuel, 2020, 270, 117469.	6.4	12

#	Article	IF	CITATIONS
91	Compositional and entropy indirect noise generated in subsonic non-isentropic nozzles. Journal of Fluid Mechanics, 2021, 910, .	3.4	12
92	Three dimensional measurements of surface areas and burning velocities of turbulent spherical flames. Combustion and Flame, 2021, 233, 111586.	5.2	12
93	Measurement of Gasoline Absorption into Engine Lubricating Oil. , 1996, , .		11
94	Spatial Analysis on Forced Heat Release Response of Turbulent Stratified Flames. Journal of Engineering for Gas Turbines and Power, 2015, 137, .	1.1	11
95	Modeling quenching distance and flame propagation speed through an iron dust cloud with spatially random distribution of particles. Journal of Loss Prevention in the Process Industries, 2016, 43, 138-146.	3.3	11
96	Flame thermometry using laser-induced-grating spectroscopy of nitric oxide. Applied Physics B: Lasers and Optics, 2018, 124, 43.	2.2	11
97	Measurement and simulation of sooting characteristics by an ATJ-SKA biojet fuel and blends with Jet A-1 fuel in laminar non-premixed flames. Combustion and Flame, 2021, 233, 111582.	5.2	11
98	Chemical Kinetic Modeling of the Oxidation of Unburned Hydrocarbons. , 0, , .		10
99	Novel Experiment on In-Cylinder Desorption of Fuel from the Oil Layer. , 0, , .		10
100	Analytical Scaling Model for Hydrocarbon Emissions From Fuel Absorption in Oil Layers in Spark Ignition Engines. Combustion Science and Technology, 1995, 109, 205-226.	2.3	10
101	Liquid Fuel Visualization Using Laser-Induced Fluoresence During Cold Start. , 1998, , .		10
102	Numerical Modeling of Fuel Sprays in DISI Engines Under Early-Injection Operating Conditions. , 0, , .		10
103	Measurements of non-reacting and reacting flow fields of a liquid swirl flame burner. Chinese Journal of Mechanical Engineering (English Edition), 2015, 28, 394-401.	3.7	10
104	Study on hybrid combustion of aero-suspensions of boron-aluminum powders in a quiescent reaction medium. Journal of Loss Prevention in the Process Industries, 2017, 49, 645-651.	3.3	10
105	Experimental and numerical study on soot formation in laminar diffusion flames of biodiesels and methyl esters. Proceedings of the Combustion Institute, 2021, 38, 1335-1344.	3.9	10
106	Particulate Matter Emission During Start-up and Transient Operation of a Spark-Ignition Engine. , 1999, , .		9
107	Measuring ultrafine aerosols by direct photoionization and charge capture in continuous flow. Aerosol Science and Technology, 2018, 52, 546-556.	3.1	9
108	Measuring aerosol active surface area by direct ultraviolet photoionization and charge capture in continuous flow. Aerosol Science and Technology, 2019, 53, 1429-1440.	3.1	9

#	Article	IF	CITATIONS
109	Numerical investigation on the generation, mixing and convection of entropic and compositional waves in a flow duct. Journal of Sound and Vibration, 2020, 472, 115155.	3.9	9
110	Experimental study of thiophene and ferrocene in synthesis of single-walled carbon nanotubes in rich premixed hydrogen/air flames. Combustion and Flame, 2022, 238, 111939.	5.2	9
111	Development of a Time and Space Resolved Sampling Probe Diagnostic for Engine Exhaust Hydrocarbons. , 1996, , .		8
112	Chemical kinetic simulation of hydrocarbon oxidation through the exhaust port of a spark ignition engine. Combustion and Flame, 1996, 107, 383-400.	5.2	8
113	Soot mass concentration sensor using quartz-enhanced photoacoustic spectroscopy. Aerosol Science and Technology, 2019, 53, 971-975.	3.1	8
114	Dust Explosion Propagation in Small Diameter Pipes. Process Safety Progress, 2019, 38, e12033.	1.0	8
115	Synthesis of single-walled carbon nanotubes in rich hydrogen/air flames. Materials Chemistry and Physics, 2020, 254, 123479.	4.0	8
116	Instantaneous flame front identification by Mie scattering vs. OH PLIF in low turbulence Bunsen flame. Experiments in Fluids, 2022, 63, .	2.4	8
117	Detailed Calculation of Heating, Evaporation, and Reaction Processes of a Thin Liquid Layer of Hydrocarbon Fuel. , 2000, , .		7
118	Flow Field of a Model Gas Turbine Swirl Burner. Advanced Materials Research, 0, 622-623, 1119-1124.	0.3	7
119	Scalar dissipation rate and scales in swirling turbulent premixed flames. Proceedings of the Combustion Institute, 2017, 36, 1957-1965.	3.9	7
120	Measurement of the effect of water droplets on strained laminar flames using two-phase PIV. Proceedings of the Combustion Institute, 2021, 38, 3183-3192.	3.9	7
121	Auto-Oil Program Phase II Heavy Hydrocarbon Study: Fuel Species Oxidation Chemistry and Its Relationship to the Auto-Oil Data. , 1994, , .		6
122	Effect of Operating Conditions and Fuel Type on Crevice HC Emissions: Model Results and Comparison with Experiments. , 0, , .		6
123	Scalar structure of turbulent stratified swirl flames conditioned on local equivalence ratio. Combustion and Flame, 2016, 166, 76-79.	5.2	6
124	Quantitative measurement of temperature in oxygen enriched CH4/O2/N2 premixed flames using Laser Induced Thermal Grating Spectroscopy (LITGS) up to 1.0â€⁻MPa. Proceedings of the Combustion Institute, 2019, 37, 1427-1434.	3.9	6
125	High Frequency Measurement of Temperature and Composition Spots With LITGS. Journal of Engineering for Gas Turbines and Power, 2019, 141, .	1.1	6
126	Gas-phase Raman spectroscopy of non-reacting flows: comparison between free-space and cavity-based spontaneous Raman emission. Applied Optics, 2019, 58, C92.	1.8	6

#	Article	IF	CITATIONS
127	Tracer-free laser-induced grating spectroscopy using a pulse burst laser at 100 kHz. Optics Express, 2019, 27, 31217.	3.4	6
128	Auto-Oil Program Phase II Heavy Hydrocarbon Study: Analysis of Engine-Out Hydrocarbon Emissions Data. , 1994, , .		5
129	Effect of Cooling Liner on Acoustic Energy Absorption and Flame Response. , 2010, , .		5
130	Spray Characteristics of an Internal-Mix Airblast Atomizer. Applied Mechanics and Materials, 0, 629, 125-130.	0.2	5
131	Direct comparison of PDF and scalar dissipation rates between LEM simulations and experiments for turbulent, premixed methane air flames. Combustion and Flame, 2016, 165, 208-222.	5.2	5
132	Evaluation of manifold representations of chemistry in stratified, swirl-stabilized flames. Combustion and Flame, 2021, 229, 111418.	5.2	4
133	Effects of Nonuniform Reactant Stoichiometry on Combustion Instability. , 2011, , .		3
134	Fundamental Spray Combustion Characteristics of Rapeseed Biodiesel, Diesel and Blend. Energy Procedia, 2015, 75, 2394-2399.	1.8	3
135	Hydrogen autoignition at pressures above the second explosion limit (0.6–4.0 MPa). International Journal of Chemical Kinetics, 1998, 30, 385-406.	1.6	3
136	Oxidation of hydrocarbons from lubricant oil layers in spark-ignition engines. Proceedings of the Combustion Institute, 1996, 26, 2645-2652.	0.3	2
137	Hydrogen production via plasma reformers. , 0, , .		2
138	Isothermal flow measurements in a gas turbine combustor using a fast flame ionization detector. Measurement Science and Technology, 2010, 21, 055107.	2.6	2
139	Investigation of the Effect of Combustor Cooling Geometry on Acoustic Energy Absorption. , 2010, , .		2
140	Effects of the Biodiesel Fuel Physical Properties on the Swirl Stabilised Spray Combustion Characteristics. , 0, , .		2
141	Uncertainty analysis in structured laser illumination planar imaging (SLIPI) applied to non-linear signals: gas-phase phosphor thermometry. Measurement Science and Technology, 2019, 30, 084003.	2.6	2
142	Comparison of Acoustic Velocity Perturbation Measurements Using PIV vs. Two-Microphone Technique. , 2013, , .		1
143	Proper Orthogonal Decomposition Analysis of Non-Swirling Turbulent Stratified and Premixed Methane/Air Flames. , 2014, , .		1
144	OxyCAP UK: Oxyfuel Combustion - academic Programme for the UK. Energy Procedia, 2014, 63, 504-510.	1.8	1

#	Article	IF	CITATIONS
145	Spatial Analysis on Forced Heat Release Response of Turbulent Stratified Flames. , 2014, , .		1
146	Application of Multiscalar Laser Diagnostics to Turbulent Stratified Methane/Air Flames. , 2008, , .		0
147	Quantitative Temperature Measurement of Toluene/air Mixture using Laser Induced Thermal Grating Spectroscopy (LITGS). The Proceedings of Mechanical Engineering Congress Japan, 2016, 2016, G0600101.	0.0	0
148	Open-source modelling of aerosol dynamics and computational fluid dynamics: bipolar and unipolar diffusion charging and photoelectric charging. Computer Physics Communications, 2022, , 108399.	7.5	0